

Latent Heat Observation of the $q=3, 4$, and 5 Potts models by Tensor Product Variational Approach

A. Gendiar^{1,2} and T. Nishino³

¹ *Institute of Physics, Slovak Academy of Sciences, Dúbravská cesta 9, SK-842 28 Bratislava, Slovakia*

² *Institute of Electrical Engineering, Slovak Acad. of Sci., Dúbravská cesta 9, SK-842 39 Bratislava, Slovakia*

³ *Department of Physics, Graduate School of Science, Kobe University, 657-8501, Japan*

(March 9, 2019)

Three-dimensional (3D) q -state Potts models ($q=3, 4$, and 5) are studied by recently developed algorithm, the tensor product variational approach (TPVA) for 3D classical lattice models. TPVA has been proposed as a self-consistent method for numerical calculations based on the density matrix renormalization group (DMRG) ideas. TPVA calculates and optimizes the variational state of a 3D transfer matrix as a 2D product of tensors. The variational partition function is calculated by the corner transfer matrix renormalization group (CTMRG). Transition points are obtained for the $q=3, 4$, and 5 state Potts models by the independent observation of the free energy, internal energy and magnetization for two various boundary conditions. Latent heats are determined for these models because they exhibit the first-order phase transitions.

05.50.+q, 75.10.Hk, 05.70.Fh, 02.70.-c

I. INTRODUCTION

In 1992 the density matrix renormalization group (DMRG) technique has been invented by White [1,2] and applied to one-dimensional (1D) quantum spin chains. Three years later, DMRG has been applied to two-dimensional (2D) classical systems by one of us [3]. DMRG has become a powerful method for a wide class of 1D quantum and 2D classical models [4].

A further DMRG improvement of the 2D classical systems is based on Baxter's corner transfer matrix [5,6]. In 1968 Baxter introduced a general formulation of the transfer matrix variational method [6] and suggested a variational trial function in a matrix product form. Moreover, he has shown that not only the transfer matrices had been suitable to consider but row-column symmetries might also have been taken into account. He invented a corner transfer matrix and created an iterative method for its solution [7,8] which could be reformulated by the self-consistent truncated equation of the corner transfer matrix and in 1996 the corner transfer matrix renormalization group (CTMRG) was developed on these ideas by one of us [9].

The variational approach seems to be the key point for further attempts how to extend DMRG to higher dimensions. The first idea based on corner transfer tensor renormalization group (CTTRG) [10], as a 3D generalization of CTMRG working in two dimensions, has not offered reliable results when tested on the simple 3D Ising model. The next considerations led to Kramers-Wannier approximation [11] where authors Okunishi and Nishino treated 3D Ising model by searching two adjustable parameters in order to construct the best 2D variational state of the model [12]. Although, the results were more precise than those coming from CTTRG, the authors have not found any correct answer yet how to ap-

ply Kramers-Wannier approximation to models differing from the Ising one.

In this paper we describe a numerical efficiency of the recently developed tensor product variational approximation (TPVA) [13,14], discuss properties and stability of the method and apply TPVA to $q=3, 4$, and 5 state Potts models. In Sec. II we introduce the models and briefly present the variational method. In Sec. III we derive the free energy, internal energy and magnetization which can be extracted from TPVA independently and in Sec. IV we discuss the stability of the algorithm for open and fixed boundary conditions. The numerical results obtained from TPVA are presented in Sec. V and in Sec. VI we conclude and discuss the numerical stability and efficiency of TPVA.

II. VARIATIONAL APPROACH

We consider the three-dimensional classical spin model of the interaction round a face (IRF) type defined on a simple cubic lattice for the q -state Potts models. The whole lattice is constructed from joined local Boltzmann weights W_B as seen in Fig. 1.

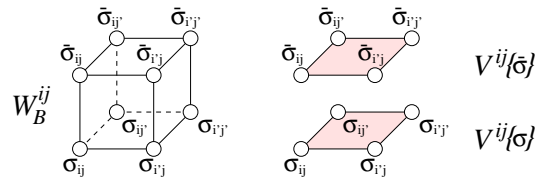


FIG. 1. A simple cubic local Boltzmann weight (IRF type) for the q -state Potts models. Variational product states $\langle\Phi|$ and $|\Psi\rangle$ are expressed by the product of 2D matrices $V^{ij}\{\bar{\sigma}\}$ and $V^{ij}\{\sigma\}$ in Eqs. (5) and (6), respectively.

The edges of the cubic W_B are occupied by q -state

variables $\sigma = 0, 1, \dots, q-1$. The bar variables $\bar{\sigma}$ always appear in the next upper layer to σ and the notations of spin positions i, j on the 2D layer are reduced here to $i' = i+1$ and $j' = j+1$.

Let us consider a cubic lattice of the size $2N \times 2N \times \infty$ in the X, Y, and Z directions, respectively, $2N \times 2N$ being the dimension (or size) of the layer-to-layer transfer matrix \mathcal{T} . The partition function \mathcal{Z} for the lattice of size $2N \times 2N \times M$ ($M \rightarrow \infty$) is then given by

$$\mathcal{Z}_{2N \times 2N \times \infty} = \lim_{M \rightarrow \infty} \text{Tr} \mathcal{T}^M \left\{ \bar{\sigma} \right\}. \quad (1)$$

Assuming ferromagnetic interactions $J < 0$ between the nearest-neighbor q -state variables $\sigma = 0, 1, \dots, q-1$ in the Potts models as well as an external magnetic field H acting on each spin site at fixed zero level, i. e., $H\delta_{0\sigma_{ij}}$ for $i = 1, 2, \dots, 2N$ and $j = 1, 2, \dots, 2N$, we can write down the local Boltzmann weight W_B^{ij} at the position i, j as

$$\begin{aligned} W_B^{ij} \left\{ \begin{array}{cccc} \bar{\sigma}_{ij} & \bar{\sigma}_{i'j} & \bar{\sigma}_{i'j'} & \bar{\sigma}_{ij'} \\ \sigma_{ij} & \sigma_{i'j} & \sigma_{i'j'} & \sigma_{ij'} \end{array} \right\} = \\ = \exp \left[\frac{-J}{4k_B T} \left(\delta_{\sigma_{ij}\sigma_{i'j}} + \delta_{\sigma_{i'j}\sigma_{i'j'}} + \delta_{\sigma_{i'j'}\sigma_{ij'}} + \delta_{\sigma_{ij'}\sigma_{ij}} \right. \right. \\ \left. \left. + \delta_{\bar{\sigma}_{ij}\bar{\sigma}_{i'j}} + \delta_{\bar{\sigma}_{i'j}\bar{\sigma}_{i'j'}} + \delta_{\bar{\sigma}_{i'j'}\bar{\sigma}_{ij'}} + \delta_{\bar{\sigma}_{ij'}\bar{\sigma}_{ij}} \right. \right. \\ \left. \left. + \delta_{\sigma_{ij}\bar{\sigma}_{ij}} + \delta_{\sigma_{i'j}\bar{\sigma}_{i'j}} + \delta_{\sigma_{i'j'}\bar{\sigma}_{i'j'}} + \delta_{\sigma_{ij'}\bar{\sigma}_{ij'}} \right) \right. \\ \left. - \frac{H}{8k_B T} \left(\delta_{0\sigma_{ij}} + \delta_{0\sigma_{i'j}} + \delta_{0\sigma_{i'j'}} + \delta_{0\sigma_{ij'}} \right. \right. \\ \left. \left. + \delta_{0\bar{\sigma}_{ij}} + \delta_{0\bar{\sigma}_{i'j}} + \delta_{0\bar{\sigma}_{i'j'}} + \delta_{0\bar{\sigma}_{ij'}} \right) \right]. \quad (2) \end{aligned}$$

Then, the transfer matrix \mathcal{T} defined on two adjacent site layers (each layer consists of $2N \times 2N$ sites) can be expressed by a product of local Boltzmann eights

$$\mathcal{T} \left\{ \bar{\sigma} \right\} = \prod_{i=1}^{2N-1} \prod_{j=1}^{2N-1} W_B^{ij}. \quad (3)$$

We follow the variational scheme where the variational states $\langle \Phi |$ and $|\Psi \rangle$ standing in the expression of the variational partition function,

$$\lambda_{\max} = \frac{\langle \Phi | \mathcal{T} \left\{ \bar{\sigma} \right\} | \Psi \rangle}{\langle \Phi | \Psi \rangle}, \quad (4)$$

can be described by TPVA in a uniform product of local tensors and it seems to be sufficient to consider a product of 2D $q \times q$ matrices $V^{ij} \{ \sigma \}$ at the lowest approximation. So far, higher approximations have been studied in the 3D vertex Ising model only [14] where the authors encountered instability for cases of $m > 2$. The Eq. (4) represents the Rayleigh ratio and the term λ_{\max} is maximized by the variational improving of the both variational states $\langle \Phi |$ and $|\Psi \rangle$.

The variational states $\langle \Phi |$ and $|\Psi \rangle$ written in the product form as

$$\langle \Phi | = \prod_{i=1}^{2N-1} \prod_{j=1}^{2N-1} V^{ij} \{ \bar{\sigma} \}, \quad (5)$$

$$|\Psi \rangle = \prod_{i=1}^{2N-1} \prod_{j=1}^{2N-1} V^{ij} \{ \sigma \} \quad (6)$$

approximate the left and right eigenstates of the 3D transfer matrix \mathcal{T} and can be later used to obtain thermodynamic functions of 3D classical lattice models with short-range interactions. Here we refer readers to Refs. [13,14] where more detailed description of the TPVA algorithm is explained.

We recall that the calculation of the $V^{ij} \{ \sigma \}$ is positionally independent in TPVA for large lattices ($N \rightarrow \infty$) and consists of two independent CTMRG algorithms both for the transfer matrix \mathcal{T} as well as for the product variational states $\langle \Phi |$ and $|\Psi \rangle$. In other words, CTMRG expands the lattice size within each iteration by 2 sites in both X and Y directions, starting from the single initial conditions $\mathcal{T} \equiv W_B$ and $\langle \Phi | \equiv |\Psi \rangle \equiv V$ (V being set up arbitrarily because the reached fixed point does not depend on any initial choice of V). The expanding transfer matrix dimension $2N \times 2N$ increases in the N -th iteration according to the following mapping $2 \times 2 \rightarrow 4 \times 4 \rightarrow 6 \times 6 \rightarrow \dots \rightarrow (2N-2) \times (2N-2) \rightarrow (2N) \times (2N) \rightarrow \dots$

III. THERMODYNAMIC FUNCTIONS

So far, the 3D classical q -state Potts models have not been exactly solved but there are some conjectures saying that for $q \geq 3$ these models exhibit the first-order phase transitions [15]. Therefore, in our calculations we should observe discontinuity in the internal energy E_{int} as a function of temperature T whereas the free energy F as a function of temperature T must remain continuous at the transition point T_t . These facts lead us to derive thermodynamic functions from TPVA such as the free energy F , the internal energy E_{int} and magnetization M per a unit cell and thus confirm by numerical calculations the above mentioned conjectures.

The partition function \mathcal{Z} defined in Eq. (1) is closely related to the free energy F per a unit cell in the thermodynamic limit through the formulae

$$\begin{aligned} F(T, H) &= -k_B T \lim_{N \rightarrow \infty} \frac{1}{(2N)^2} \ln \mathcal{Z}_{2N \times 2N \times \infty} \\ &= -k_B T \lim_{N \rightarrow \infty} \ln (\lambda_{\max})^{\frac{1}{2N}} \\ &= -k_B T \lim_{N \rightarrow \infty} \ln \left(\frac{\langle \Phi_{2N} | \mathcal{T}_{2N} | \Psi_{2N} \rangle}{\langle \Phi_{2N} | \Psi_{2N} \rangle} \right)^{\frac{1}{2N}} \quad (7) \end{aligned}$$

where the number of CTMRG iterations as well as the dimension of the system are both described by the same term N . The free energy F is normalized in each iteration

in order to observe its convergence at finite N . We identify this converged state with the thermodynamic limit ($N \rightarrow \infty$) due to the fixed precision of numerical calculations.

Let us introduce F_N to be the free energy of an $2N \times 2N$ square system, i. e.,

$$F_N = -k_B T \left[f_2(2N)^2 + f_1(2N) + f_0 + \mathcal{O}(N^{-1}) \right], \quad (8)$$

where we have taken into account a surface energy and higher corrections. TPVA computes both $\langle \Phi_{2N} | \Psi_{2N} \rangle$ and $\langle \Phi_{2N} | \mathcal{T}_{2N} | \Psi_{2N} \rangle$ simultaneously by use of corner transfer matrices C_{2N} and D_{2N} , respectively [9,11]. In order to accelerate the numerical convergence of the free energy with respect to N , we avoid to use Eq. (7) and derive a new formula instead. The Reyleigh ratio in Eq. (4) represents the partition function per a layer and applying Eq. (8) to the Reyleigh ratio, the following expressions are then satisfied: for the numerator

$$\begin{aligned} \langle \Phi_{2N} | \mathcal{T}_{2N} | \Psi_{2N} \rangle &= \text{Tr} \{ D_N^4 \} \\ &= \exp \left\{ B_2(2N)^2 + B_1(2N) + B_0 + \mathcal{O}(N^{-1}) \right\} \end{aligned} \quad (9)$$

and for the denominator

$$\begin{aligned} \langle \Phi_{2N} | \Psi_{2N} \rangle &= \text{Tr} \{ C_N^4 \} \\ &= \exp \left\{ A_2(2N)^2 + A_1(2N) + A_0 + \mathcal{O}(N^{-1}) \right\}. \end{aligned} \quad (10)$$

Let us consider the following relations

$$\begin{aligned} \mathcal{B}_{2N} &= \frac{\langle \Phi_{2N-2} | \mathcal{T}_{(2N-2)} | \Psi_{2N-2} \rangle \langle \Phi_{2N+2} | \mathcal{T}_{(2N+2)} | \Psi_{2N+2} \rangle}{\langle \Phi_{2N} | \mathcal{T}_{2N} | \Psi_{2N} \rangle \langle \Phi_{2N} | \mathcal{T}_{2N} | \Psi_{2N} \rangle} \\ &= \exp \{ 8B_2 \}, \end{aligned} \quad (11)$$

$$\mathcal{A}_{2N} = \frac{\langle \Phi_{2N-2} | \Psi_{2N-2} \rangle \langle \Phi_{2N+2} | \Psi_{2N+2} \rangle}{\langle \Phi_{2N} | \Psi_{2N} \rangle \langle \Phi_{2N} | \Psi_{2N} \rangle} = \exp \{ 8A_2 \}, \quad (12)$$

as they do not depend on the lattice size N up to the higher-term corrections $\mathcal{O}(N^{-1})$. Hence, we apply accelerated formula for the numerical calculation of the free energy $F(T, H)$ per a unit cell

$$F(T, H) = -\frac{1}{8} k_B T \lim_{N \rightarrow \infty} \ln \left(\frac{\mathcal{B}_{2N}}{\mathcal{A}_{2N}} \right). \quad (13)$$

The internal energy E_{int} per unit cell is known as the first derivative of the free energy per unit cell F with respect to temperature T (i.e., $E_{\text{int}} = -T^2 \frac{\partial}{\partial T} [F/T]$) and this definition is in TPVA equivalent to

$$E_{\text{int}} = -\langle \delta_{\sigma_{ij} \sigma_{i'j'}} \rangle - \langle \delta_{\sigma_{ij} \sigma_{ij'}} \rangle - \langle \delta_{\sigma_{ij} \bar{\sigma}_{ij}} \rangle. \quad (14)$$

Analogously, the magnetization per unit cell $M = \frac{\partial}{\partial H} F(T, H)$ can be numerically calculated through the following expression

$$M = \frac{q \langle \delta_{0\sigma_{ij}} \rangle - 1}{q - 1}, \quad (15)$$

where q corresponds to the q value in the q -state Potts model. The terms $\langle \delta_{\sigma\sigma'} \rangle$ in Eqs. (14) and (15) represent average values of the nearest-neighbor $\langle \delta_{\sigma\sigma'} \rangle$ correlations, i. e.,

$$\langle \delta_{\sigma\sigma'} \rangle = \frac{\langle \Phi | \delta_{\sigma\sigma'} \mathcal{T} | \Psi \rangle}{\langle \Phi | \Psi \rangle}. \quad (16)$$

IV. STABILITY OF THE TPVA ALGORITHM

All above mentioned thermodynamic functions, yielded from the TPVA calculations, have converged fast after several hundreds of CTMRG iterations (up to $N=500$). Throughout the iterations, the treated models behave similarly as is well-known in DMRG, i. e., the models undergo spontaneous symmetry breaking and select one of the two possible free energy minima. This behavior is the most significant for the open (or free) boundary conditions (OBC) in TPVA and measured magnetization M per unit cell varies slowly from $M=0$ to some fixed nonzero value in the ordered phase (M remains zero in the disordered phase). The spontaneous symmetry breaking is caused by numerical fluctuations coming from the initial setting of matrix V (i. e., from the self-consistent improving in subsequent optimizations of the variational states $\langle \Phi |$ and $| \Psi \rangle$) as well as from the renormalizations process. The both reasons are equivalent to a small external magnetic field H added to Hamiltonian of the model.

In order to speed up the TPVA convergence in the ordered phase, the external magnetic field H was inserted to the Boltzmann weight definition in Eq. (2). We set up small nonzero field H at the very beginning of the TPVA calculation and after several iteration steps ($N \leq 10$), we set $H=0$. This is equivalent to the fixed boundary conditions (FBC). We apply OBC and FBC to the q -state Potts model because OBC stabilizes the presence of the disordered phase and FBC stabilizes the ordered phase in the particular model.

Now, let us discuss the stability of TPVA. The self-consistent equation optimizing the variational states $\langle \Phi |$ and $| \Psi \rangle$ requires an improvement. The original formulation [13] improved $V\{\sigma\}$ directly and might lead the TPVA algorithm to instability. Therefore, we had to introduce a small parameter ε to slow down the improvement of the matrix $V\{\sigma\}$ from $V^{\text{old}}\{\sigma\}$ to $V^{\text{new}}\{\sigma\}$, in particular,

$$V^{\text{new}}\{\sigma\} \leftarrow \|V^{\text{old}}\{\sigma\} + \varepsilon V^{\text{new}}\{\sigma\}\|_{\text{norm}} \quad (17)$$

where $\|\cdot\|_{\text{norm}}$ represents the normalization. Thus modified TPVA remains always stable for $\varepsilon \leq 0.1$.

Too strong external magnetic field $|H| \geq 0.1$ sometimes causes instability around the transition point T_t , since

the ground state and the first excited state are almost degenerated in the close vicinity of T_t . Thus, the strong magnetic field H can shift the transition point to higher values and the first excited state may be caught instead.

V. NUMERICAL RESULT

We treat thermodynamic properties of the 3D classical ferromagnetic q -state Potts models near the transition point K_t (K being the inverse temperature, i. e., $K \equiv T^{-1}$). Throughout all numerical TPVA calculations, we kept fixed the multi-state variable $m=20$ [13,14], parameter $\varepsilon=0.1$ and the external magnetic field H varies within the interval $H \in \langle 0.0001, 0.01 \rangle$ both for $q=3$ and $q=4$ state Potts models.

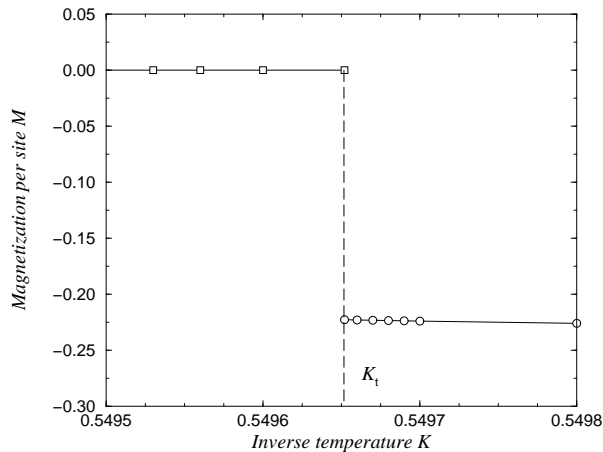


FIG. 2. The discontinuity of the magnetization per spin M versus inverse temperature K in the $q=3$ state Potts model near the transition. Below transition point K_t , the zero magnetization points out the disordered phase and above K_t , there is the ordered phase.

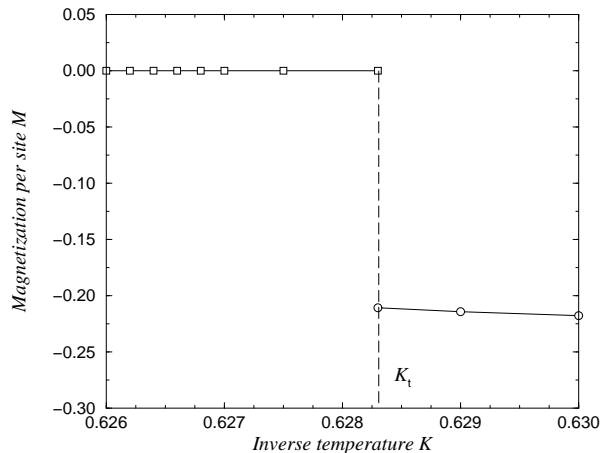


FIG. 3. The magnetization per spin M vs. inverse temperature K for the $q=4$ state Potts model.

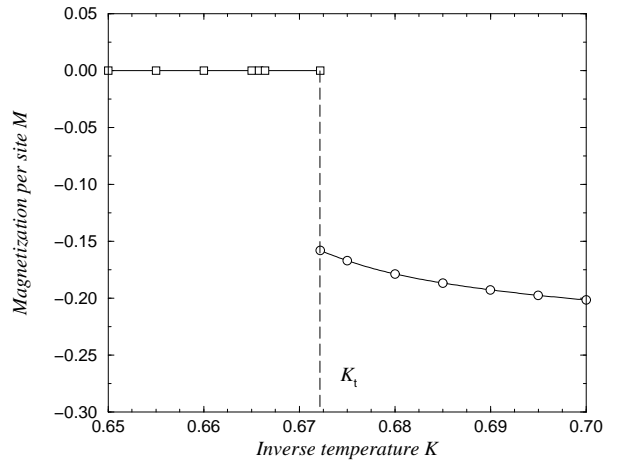


FIG. 4. The magnetization per spin M vs. inverse temperature K for the $q=5$ state Potts model.

Calculated spontaneous magnetizations per spin M for the $q=3, 4$, and 5 Potts models at the center of the $2N \times 2N \times \infty$ lattice size are shown in Figs. 2, 3, and 4, respectively. We emphasize the discontinuity of the spontaneous magnetization M as the function of inverse temperature K at the transition point K_t .

TPVA yields the transition point $K_t^{[q=3]} = 0.549562$ for the $q=3$ state Potts model which is only 0.18% lower than the Monte Carlo result $K_t^{\text{MC}} = 0.550565 \pm 0.000010$ [16]. In the cases of the $q=4$ and 5 state Potts models, the calculated transition points yield $K_t^{[q=4]} = 0.6283$ and $K_t^{[q=5]} = 0.6722$, respectively.

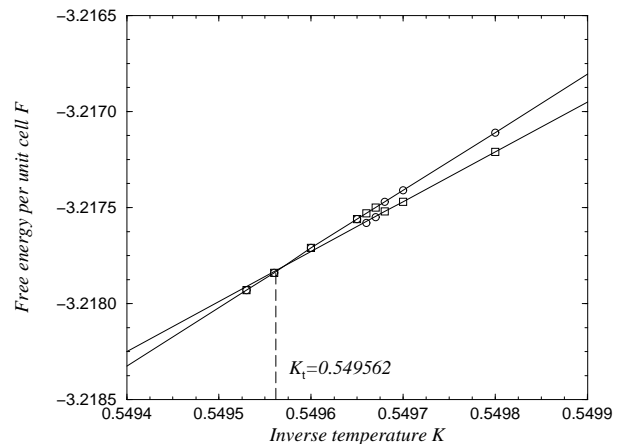


FIG. 5. The free energy per unit cell F as the function of K for OBC and FBC for the $q=3$ state Potts model. Squares and circles represent data obtained by TPVA calculation through the Eq. (13) for OBC and FBC, respectively. Additional extrapolation of the data for FBC were performed to localize the transition point K_t as the free energy crossover.

We have determined the transition points by the detailed studies of the free energy F per unit cell for both open and fixed boundary conditions. Corresponding graphs of the free energies F versus inverse temperature

K are depicted in Figs. 5, 6 and 7 for $q = 3, 4$, and 5, respectively. The squares and circles represent OBC and FBC, respectively. Due to the presence of degeneracy of the ground state and the first excited state at the transition point K_t , we have obtained slightly different free energies F for OBC and FBC near K_t . Therefore, we determine the transition point K_t as the free energy crossover of both F^{OBC} and F^{FBC} .

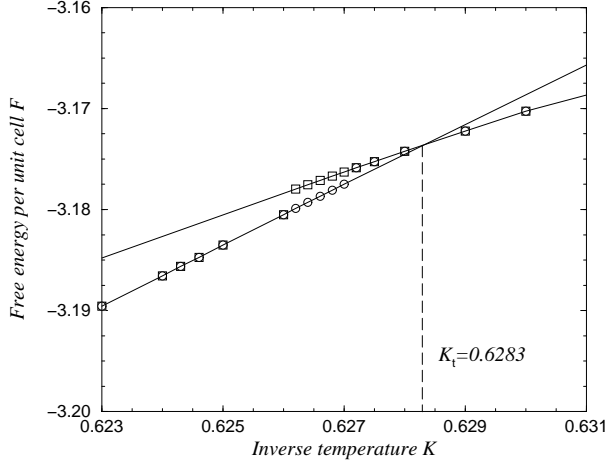


FIG. 6. The free energy per unit cell F as the function of K for OBC and FBC for the $q=4$ state Potts model. Squares and circles represent data for OBC and FBC, respectively. The transition point K_t is determined by the extrapolation of the free energy data.

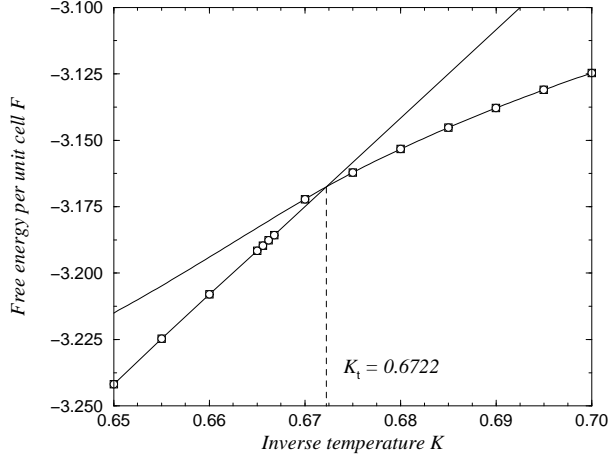


FIG. 7. The free energy per unit cell F as the function of K for OBC and FBC for the $q=5$ state Potts model.

In Figs. 8, 9, and 10, we have plotted the internal energy per bond e_{int} [17] as the function of the inverse temperature K . The internal energy gap points out the existence of the first order phase transition for the all 3D $q=3, 4$, and 5 state Potts models. The latent heat [16]

$$l = 3(e_{\text{int}}^+ - e_{\text{int}}^-) = (E_{\text{int}}^+ - E_{\text{int}}^-) \quad (18)$$

is proportional to the internal energy gap. The ener-

gies E_{int}^+ and E_{int}^- are extrapolated values of the E_{int} towards the transition point K_t obtained from the free energy crossover. For the $q=3$ state Potts model, the latent heat obtained by numerical Monte Carlo simulations yields $l_{\text{MC}} = 0.16160 \pm 0.00047$ which is differing about 41% than our result $l = 0.2280$. All numerical results obtained from TPVA are summarized in Table I.

TABLE I. Numerically obtained transition points K_t and latent heats l by TPVA for the 3D ferromagnetic $q=3, 4$, and 5 state Potts models. The parameter m denotes the multi-state variable well-known from DMRG (Refs. 1-4).

q	m	K_t	l
3	20	0.549562	0.2280
4	20	0.6283	0.6189
5	5	0.6722	0.693

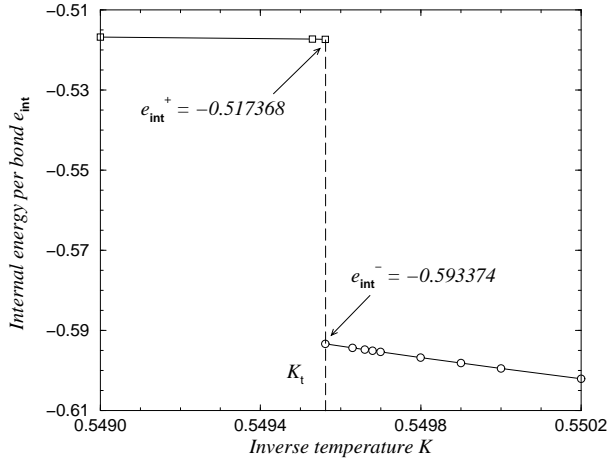


FIG. 8. The internal energy e_{int} per bond (Ref. 17) vs. K for the $q=3$ state Potts model. The precise determination of e_{int}^+ and e_{int}^- comes from the extrapolation of the internal energy towards the correct transition point K_t determined by the free energy crossover.

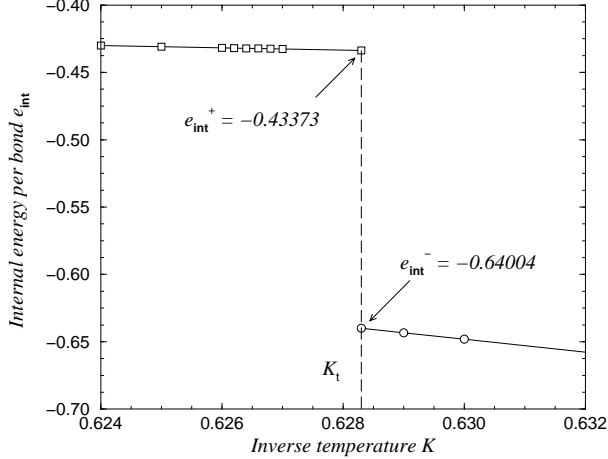


FIG. 9. The internal energy e_{int} per bond vs. K for the $q=4$ state Potts model.

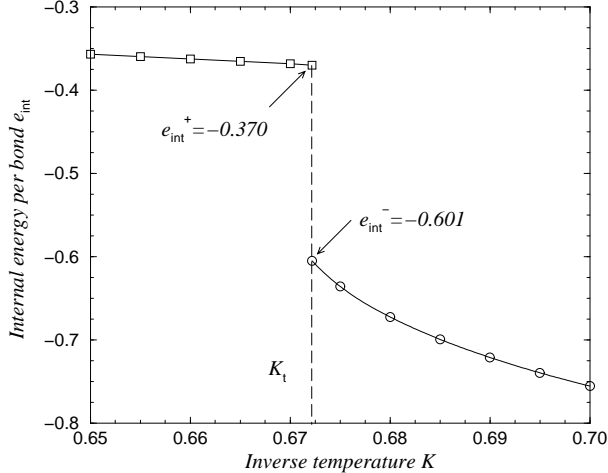


FIG. 10. The internal energy e_{int} per bond vs. K for the $q=5$ state Potts model.

VI. CONCLUSIONS AND DISCUSSIONS

Recently proposed self-consistent TPVA algorithm has been applied to more complicated 3D classical $q=3, 4$, and 5 state Potts models and we stressed our interests to universality and stability of TPVA. We have shown that the algorithm is suitable for studying larger class of models. We have derived several thermodynamic functions that are of use for any other models. We have confirmed the stability of TPVA by studying of the q -state Potts models and it has been shown that TPVA remained stable for the external magnetic fields $|H| \leq 0.01$ and the parameters $\varepsilon \leq 0.1$.

We have obtained the transition points K_t and the latent heats l for the $q=3, 4$, and 5 state Potts models. We were able to confirm the first-order phase transitions for these not analytically solvable models through the observation of the free energy F as well as through the discontinuity of the internal energy E_{int} and the spontaneous magnetization M .

ACKNOWLEDGMENTS

T. N. thanks to Y. Hieida, K. Okunishi, N. Maeshima, and Y. Akutsu for discussions about tensor product formulations. This work has been partially supported by the Slovak Grant Agency, VEGA No. 2/7174/20 and Grant-in-Aid for Scientific Research from Ministry of Education, Science, Sports and Culture (No. 09640462 and No. 11640376). The numerical calculations were performed by Compaq Fortran on the HPC-Alpha UP21264 Linux workstation.

-
- [1] S.R. White, Phys. Rev. Lett. **69** (1992), 2863.
 - [2] S.R. White, Phys. Rev. B **48** (1993), 10345.
 - [3] T. Nishino, J. Phys. Soc. Jpn. **64** (1995), 3598.
 - [4] *Density-Matrix Renormalization — A New Numerical Method in Physics*, Lecture notes in Physics, eds. I. Peschel, X. Wang, M. Kaulke, and K. Hallberg (Springer Verlag, 1999).
 - [5] R. Baxter, J. Math. Phys. **9** (1968), 650; J. Stat. Phys. **19** (1978), 461.
 - [6] R.J. Baxter, *Exactly Solved Models in Statistical Mechanics* (Academic Press, London, 1982), p.363.
 - [7] R. J. Baxter and I. G. Enting, J. Stat. Phys. **21** (1979), 103.
 - [8] R. J. Baxter, I. G. Enting, and S. K. Tsang, J. Stat. Phys. **22** (1980), 465.

- [9] T. Nishino and K. Okunishi, J. Phys. Soc. Jpn. **65** (1996), 891; J. Phys. Soc. Jpn. **66** (1997), 3040.
- [10] T. Nishino and K. Okunishi, J. Phys. Soc. Jpn. **68** (1999), 3066.
- [11] H.A. Kramers and G.H. Wannier, Phys. Rev. **60** (1941), 263.
- [12] K. Okunishi and T. Nishino, Prog. Theor. Phys.**103** (2000), 541.
- [13] T. Nishino, K. Okunishi, Y. Hieida, N. Maeshima and Y. Akutsu, Nucl. Phys. B **575** (2000), 504.
- [14] T. Nishino, K. Okunishi, Y. Hieida, N. Maeshima, Y. Akutsu, and A. Gendiar, Prog. Theor. Phys. **105** (2001) in press (cond-mat/0011103).
- [15] F. Y. Wu, Rev. of Mod. Phys **54** (1982), 235.
- [16] W. Janke and R. Villanova, Nucl. Phys. B **489** (1997) 679.
- [17] The internal energy per bond e_{int} is related to the internal energy per unit cell E_{int} through the expression $e_{\text{int}} = \frac{1}{3}E_{\text{int}}$.